Heliyon 8 (2022) e08932

Contents lists available at ScienceDirect

Heliyon

journal homepage: www.cell.com/heliyon

Research article

Preliminary sizing of solar district heating systems with seasonal water thermal storage

Daniel P. Hiris, Octavian G. Pop, Mugur C. Balan *

Technical University of Cluj-Napoca, Romania

ARTICLE INFO

Keywords:
Solar district heating
Seasonal thermal storage
Preliminary sizing
Web based application
Aperture area
Storage system volume

ABSTRACT

The study proposes a method for preliminary and estimative sizing of the main components of solar district heating systems, with seasonal thermal storage. The main parameters determined by this method, are the aperture area of the solar thermal collectors and the volume of the seasonal thermal storage. The proposed method is only estimative, but it provides the necessary input data for the investigation ofthe dynamic thermal behavior of such systems. The main advantage of the method is that it requires only very few and accessible input data. Two situations are considered: the first in which available climatic data such as annual global solar radiation on horizontal plane and annual average temperature can be used in calculations, and the second in which such data is not available and should be determined through interpolation. With the proposed interpolation functions the annual global solar radiation on horizontal plane, the annual average temperature and the annual global efficiency of the solar thermal collectors were determined. The errors of the estimations are ranging within the intervals of (−15.6 … +25.8) % for annual global solar radiation on horizontal plane and (−10.8 … 19.1) % for annual global efficiency of the solar thermal collectors. The maximum deviations for the annual average temperature estimations were (−4.23 … +5.37) °C. With this limited accuracy, the proposed interpolation functions can be used for latitudes between (0–70) °, annual global solar radiation on horizontal plane between (704–2337) kWh/m^2/year and annual average temperatures ranging within the interval of (2–30) °C.

1. Introduction

The solar district heating systems (SDHS) are important technological achievements designed with the assumed purpose to reduce the global CO_2 emissions for both heating and domestic hot water (DHW) preparation. Since the early 1980s, the number of SDHSs and of installed capacity was continuously growing, up to over 400 large scale systems, counting almost 2.5 million m^2 of solar thermal collectors (STC) with a total capacity of more than 1600 MW [1]. Initially, the growth of this sector was driven by Europe, but in the last years the most important contribution came from outside Europe, where many more new systems were installed.

Based on the processed data available in [1], Figures 1 and 2 present the timeline evolution of the total number of systems and of the total surface area of STC respectively, both in and outside Europe, until the end of 2019.

The world's leading country in the SDHS field is Denmark, while outside Europe the most important achievements belong to China, as can be observed in Table 1, that presents the most important contributing countries and regions, the total collectors' surface area, the total thermal powers, and the total number of installed systems, at the end of 2019 [1, 2].

The capacities installed in different countries are presented in Figure 3.

The main constructive and technical characteristics of 20 SDHSs considered representatives, being located at latitudes in the range (29.77–57.87) °, in 8 countries and built in the period (1988–2019), are presented in the Tables 2 and 3, respectively.

Many studies are dedicated to SDHSs or to the integration of the SDHSs in district heating networks (DHNs), usually in combination with other heat sources. The problem of both sizing and optimization of SDHSs or of DHNs including the solar thermal subsystem is investigated in [22, 23]. In [22]a multi-objective mixed integer linear programming model, capable to perform optimal selection of technologies and capacities to be combined in DHNs is presented, while [23] presents an optimization model for both sizing and operation of a DHN based also on mixed integer linear programming and developed in MATLAB. Besides other components, both models are capable of sizing solar thermal systems and seasonal thermal storage (STS).

* Corresponding author.
E-mail address: mugur.balan@termo.utcluj.ro (M.C. Balan).

https://doi.org/10.1016/j.heliyon.2022.e08932
Received 13 September 2021; Received in revised form 1 December 2021; Accepted 7 February 2022

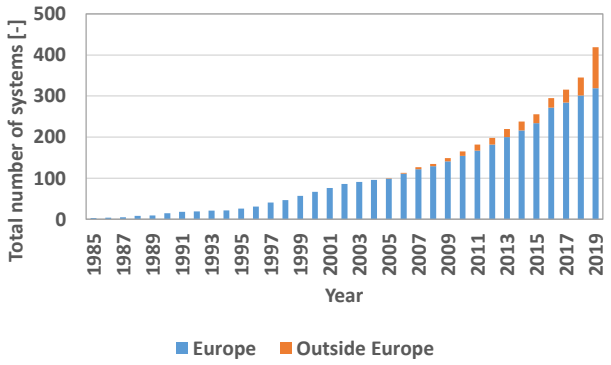

Figure 1. The timeline evolution of the total number of systems.

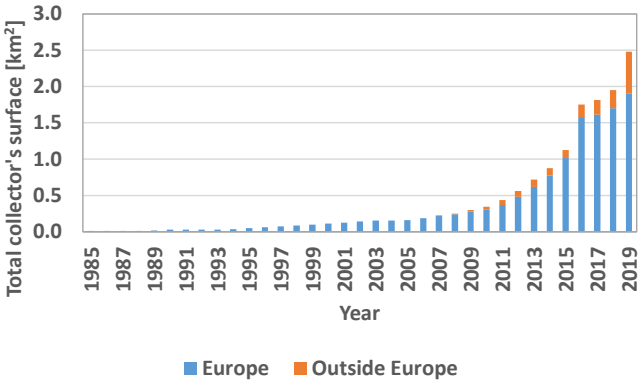

Figure 2. The timeline evolution of the area of solar thermal collectors.

Table 1. The most important contributing countries and regions in the SDHS field at the end of 2019.

Country/Region	Collector's area [m^2]	Capacity [MW]	Number of systems [-]
DNK	1,554,973	1,089.0	123
CHN	380,000	252.0	64
DEU	80,000	55.9	40
OTH European	45,000	31.1	12
Austria	44,000	30.0	28
MENA countries*	43,000	28.2	5
SWE	41,000	26.5	25
POL	24,000	16.3	15
Asia without China	23,000	14.4	13
FRA	22,500	13.0	18
NLD	22,000	11.4	8
GRC	17,000	10.1	13
CHE	16,000	8.9	13
ESP	10,000	6.2	11
USA/CAN	8,000	3.5	3
Latin America	5,000	2.7	2
ITA	4,000	1.5	3
AUS	2,000	0.5	1
ZAF	1,000	0.4	1

* Jordan, Kuwait, Dubai and Saudi Arabia.

The study [24] is dedicated to the evaluation of the feasibility and of the decarbonization cost, using STS coupled with solar thermal systems and heat pumps, in different configurations, using models to simulate the hourly energy flows. The models also include modules for economic analysis. The design of a SDHS also coupled with heat pumps is approached in [25] and the proposed mathematical model is developed as linked software packages, implemented in TRNSYS with a detailed finite element method-based model for thermal losses in the storage tank.

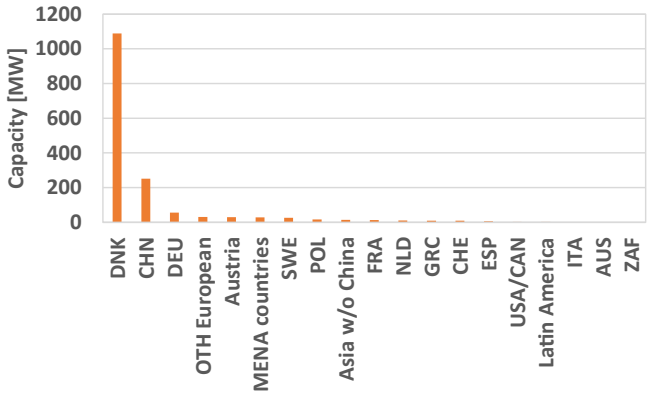

Figure 3. Capacities of SDHS installed at the end of 2019.

Some studies are dedicated to STSs in combination with different types of energy sources, other than solar energy. The review [20] is dedicated to STSs, coupled mainly with heat pumps, for both heating and cooling. It is mentioned that the STS selection is realized with complex commercial simulation software like: TRNSYS, MINSUN, Solarthermie-2000, and SOLCHIPS. In [26], the investigation is dedicated to STSs required for industrial waste-heat utilization in district heating.

According to the study [26], there is a lack of sizing approaches for STSs in the literature, that take into account both the optimal control and the dynamic behavior of the system, including the DHN. Thus, a dynamic model for the sizing of STS, developed in the modeling language Modelica, is proposed.

The common characteristics of all these models, are the great number of input data and the high complexity, because the sizing of solar district heating systems with seasonal thermal storage (SDHSSTS), is a complex and laborious task that requires a deep analysis of the installations. However, this investigation must begin with an initial basic configuration of the most important components that must be determined: the area of the STC and the volume of the STS. A simple and fast procedure for preliminary sizing of such systems is missing from the literature.

Flat solar collectors are most commonly employed in Europe while in China the evacuated tube collectors are preferred, considering, also, that it is the leading manufacturer in the field [2]. In this study, both technologies are investigated.

The use of evacuated tube collectors in China, mainly due to their economic advantages, is considered the major reason of China's leading position in the field [27].

In China, evacuated tube collectors are cheaper than flat collectors [27, 28]. Some of the technological advantages of the evacuated tube collectors over the flat collectors are the followings:

- Higher efficiency [29];
- Higher specific heat production at the same absorption area, mainly in the colder periods [29];
- Lower heat loss coefficients [27];
- Better anti-freezing behavior [27];
- Higher operating temperatures [30].

Regarding the STS, the first storage systems used insulated water tanks, usually mounted underground [15, 31], but in recent years, as the size and capacity of these systems increased, insulated pits filled with

Table 2. The main constructive characteristics of some representative SDHSs

No.	Location	Country	Latitude [°]	Year	Collectors	Storage	References
1	Vojens	DNK	55.25	2015	Flat	Pit	[3]
2	Zhongba	CHN	29.77	2019	Flat	Tank	[4]
3	Büsingen	DEU	47.70	2013	Flat	Tank	[5]
4	Dronninglund	DNK	57.16	2013	Flat	Pit	[3]
5	Nykobing	DNK	34.59	2014	Flat	Tank	[3]
6	Gram	DNK	55.29	2014	Flat	Pit	[3, 6]
7	Silkeborg	DNK	56.18	2016	Flat	Tank	[7, 8, 9]
8	Trustrup-Lyngby	DNK	56.37	2016	Flat	Tank	[9]
9	Salaspils	LVA	56.86	2019	Flat	Tank	[3, 10, 11]
10	La Parreña	MEX	31.11	2016	Flat	Tank	[3]
11	Okotoks	CAN	50.73	2008	Flat	Tank + Boreholes	[12]
12	Baotou	CHN	40.66	2017	Parabolic trough	Tank	[3]
13	Chemnitz	DEU	50.83	2000	Evacuated	Pit	[3, 12, 13, 14, 15]
14	Beijing	CHN	39.89	2017	Flat	Pit	[16]
15	Ingelstad	SWE	56.75	1988	Flat	Tank	[17]
16	Kungälv	SWE	57.87	2000	Flat	Tank	[18]
17	Herlev	DNK	55.73	1991	Flat	Tank	[15, 19]
18	Gaziantep	TUR	37.07	NA	Flat	Tank	[20]
19	Steinfurt	DEU	52.15	1998	Flat	Pit	[13, 14, 21]
20	Eggenstein	DEU	49.08	2008	Solar roof	Pit	[3, 12, 14, 15]

Table 3. The main technical characteristics of some representative SDHSs

No.	Location	I_{gh} [W/m^2]	SF [%]	Q_t [MWh/year]	Q_s [MWh/year]	A [m^2]	V [m^3]	η [%]
1	Vojens	946	45%	61778	27800	69500	203000	42.3%
2	Zhongba	1196	90%	22222	20000	34650	1000	48.3%
3	Büsingen	1192	14%	4185	565	1090	NA	43.5%
4	Dronninglund	1005	40%	37500	15000	37573	61700	39.7%
5	Nykobing	1048	19%	50210	9540	20084	6000	45.3%
6	Gram	954	61%	30000	18300	44800	122000	42.8%
7	Silkeborg	991	20%	400000	80000	156694	256000	51.5%
8	Trustrup-Lyngby	1018	30%	13377	4013	7245	2800	54.4%
9	Salaspils	969	20%	60000	12000	21595	8000	57.4%
10	La Parreña	2130	58%	7586	4400	6270	660	32.9%
11	Okotoks	1210	80%	1000	800	2307	10156	28.7%
12	Baotou	1608	33%	249973	82491	93000	66000	55.2%
13	Chemnitz	1042	42%	573	241	540	1955	42.8%
14	Beijing	NA	100%	8350	8350	10834	80000	50.3%
15	Ingelstad	924	50%	920	460	1425	5000	34.9%
16	Kungälv	977	4%	128571	4500	11000	1000	41.9%
17	Herlev	985	35%	1256	440	1025	3000	43.5%
18	Gaziantep	1837	83%	4000	3320	4000	13000	45.2%
19	Steinfurt	1052	34%	325	111	510	1000	20.6%
20	Eggenstein	1185	40%	810	324	1000	3000	27.4%

I_{gh} – Total global solar radiation on a horizontal plane; SF – Solar fraction;
Q_t – Total yearly heat load; Q_s – Useful heat provided by the solar field;
A – Area of the solar field; V – Storage volume; η – Global yearly collectors' efficiency.

water or with water and other materials like sand or gravel were used more often [15, 32, 33]. Another common thermal storage system consists of boreholes [32, 33]. In this study mainly the water-based STSs are considered.

Throughout the years, several methods were investigated for sizing the main components and for simulating the thermal behavior of solar heating systems with STS. The applications range from single houses to large districts, communities or even cities. The main input and output parameters, together with different calculation methods related to SDHS with STS are presented in Tables 4 and 5, respectively.

In this study, fully mixed STSs (without stratification) were considered and modelled. For this preliminary sizing method, this model was considered sufficiently precise according to [39, 41].

Three of the presented SDHSSTS sizing methods were implemented in commercial or free software programs [34, 40, 43]. The common characteristics of these three software programs are the following:

Table 4. The main input parameters used in the calculation methods related to solar heating with STS.

Reference	Year	Q_T	Q_s	Q_{DHW}	I_{gh}	$I_{gh,M}$	t_a	A	RVA	V	η_0	k_1	k_2	γ_t	t_f	t_r	UA	t_s	Op
[34]*	1976	-	✓	✓	✓	-	✓	✓	✓	-	✓	-	-	✓	✓	✓	✓	-	-
[35]	1977	-	-	-	-	-	-	✓	-	✓	-	-	-	-	-	-	✓	-	-
[36]	1979	✓	-	-	✓	-	✓	✓	-	✓	✓	✓	✓	-	✓	✓	✓	-	-
[37]	1980	✓	-	-	-	-	-	-	-	-	-	-	-	-	✓	✓	✓	✓	-
[38]	1980	-	-	-	✓	✓	-	-	-	-	-	-	-	-	-	-	-	-	-
[39]	1981	✓	-	-	✓	-	✓	✓	-	✓	✓	✓	✓	✓	-	-	-	✓	-
[40]**	2013	✓	-	-	✓	-	✓	✓	✓	-	✓	✓	✓	✓	✓	✓	-	✓	-
[41, 42, 43, 44, 45]***	2014–2016	✓	-	-	✓	-	✓	✓	-	-	✓	✓	✓	✓	✓	✓	✓	✓	-
[46]	2016	-	-	-	-	-	-	-	-	-	-	-	-	-	-	-	-	-	✓
[47]	2019	-	-	-	✓	-	✓	✓	-	✓	-	-	-	-	-	-	-	-	-
[48]	2019	-	✓	✓	-	-	-	✓	-	✓	✓	✓	✓	✓	-	-	-	-	-

* Implemented in commercial software (f-chart);
** Implemented in free software (SDH online calculator);
*** Implemented in free software (Simple method).

Table 5. The main output parameters and characteristics of the calculation methods related to solar heating with STS.

Reference	Year	SF	Q_{sol}	Q_{st}	t_s	A	V	η	τ	Method	Obs.
[34]*	1976	✓	✓	✓	-	-	-	-	Monthly	Analytic	Single house
[35]	1977	✓	-	-	-	-	-	-	-	Correlation	-
[36]	1979	-	-	✓	✓	-	-	-	Hourly	Analytic	Single house
[37]	1980	-	-	-	-	✓	✓	-	Monthly	Analytic	Single house
[38]	1980	-	-	-	-	-	-	✓	Daily/15 days	Analytic	50 houses
[39]	1981	✓	✓	-	✓	-	-	-	Monthly	TRNSYS	Single house
[40]**	2013	✓	✓	✓	-	-	✓	✓	NA	TRNSYS	District
[41, 42, 43, 44, 45]***	2014–2016	✓	✓	✓	✓	-	-	-	Monthly	Analytic	District
[46]	2016	-	-	✓	✓	-	-	-	Hourly	TRNSYS	District
[47]	2019	-	✓	✓	✓	-	-	✓	Hourly	TRNSYS	Hotel
[48]	2019	-	✓	✓	-	-	-	-	NA	TRNSYS	District

* Implemented in commercial software (f-chart);
** Implemented in free software (SDH online calculator);
*** Implemented in free software (Simple method).

- All of them require the solar field and the storage sizes as input data.
- All of them should be used iteratively to optimize the solar field size and the storage capacity.

Considering these aspects, the three existing software programs can be considered tools for optimization rather than sizing.

The most common input parameters of the presented methods for the study of SDHSSTS are the global solar radiation on horizontal plane, the ambient temperature, the characteristics of the STC, the tilt angle and the thermal regime of the STS and of the heating network, more precisely flow and return temperature. The large solar system should always be oriented towards the equator (South in the Northern hemisphere and North in the Southern hemisphere) [49].

Research instruments, both analytical and simulation methods, are reported and successfully used in the literature. For simulations, the most commonly used software is TRNSYS, which is very versatile and perfectly adapted for the investigation of solar heating systems with STS.

The meteorological data required for the sizing of SDHSSTS are the annual global solar radiation on horizontal plane, (I_{gh} [kWh/m^2/year]) in the considered location and the annual average temperature (t_a [°C]).

These parameters are common data that can easily be determined free of cost, as typical meteorological year (TMY) in many locations worldwide, with specialized web-based tools developed in Europe [50] or in the USA [51], as suggested in Figures 4 and 5, respectively.

The colored regions on the two maps represent the regions with available TMY. It can be observed that important regions suitable for SDHSSTS, from Australia, Canada, China, Russia, Alaska, South America, etc., are not covered by these tools.

The goal of this study is to present a preliminary sizing method dedicated to the SDHSSTS, based on very few and accessible input data. To the best of our knowledge, such a method is missing from the literature. The main computed values are the aperture area of the STC and the volume of the STS. Estimations of investments in the STC and STS are also provided. Following this step, the final sizing procedure is necessary to continue with a detailed investigation of the dynamic behavior of the system, under the most realistic conditions possible, to determine the design values of the two mentioned key parameters. This investigation can be done with the existing software optimization tools.

The usefulness and the uniqueness of the proposed preliminary sizing method consists in:

- The simplest available set of input data, in comparison to other available methods
- The capability to provide first guesses for the solar field surface area and the STS volume.

To the best knowledge of the authors, such an algorithm is missing from the literature.

The required input data of the proposed algorithm are: the annual heating demand of the consumers (Q_d [MWh/year]), the solar fraction (SF [%]), the global annual solar radiation on horizontal plane and the

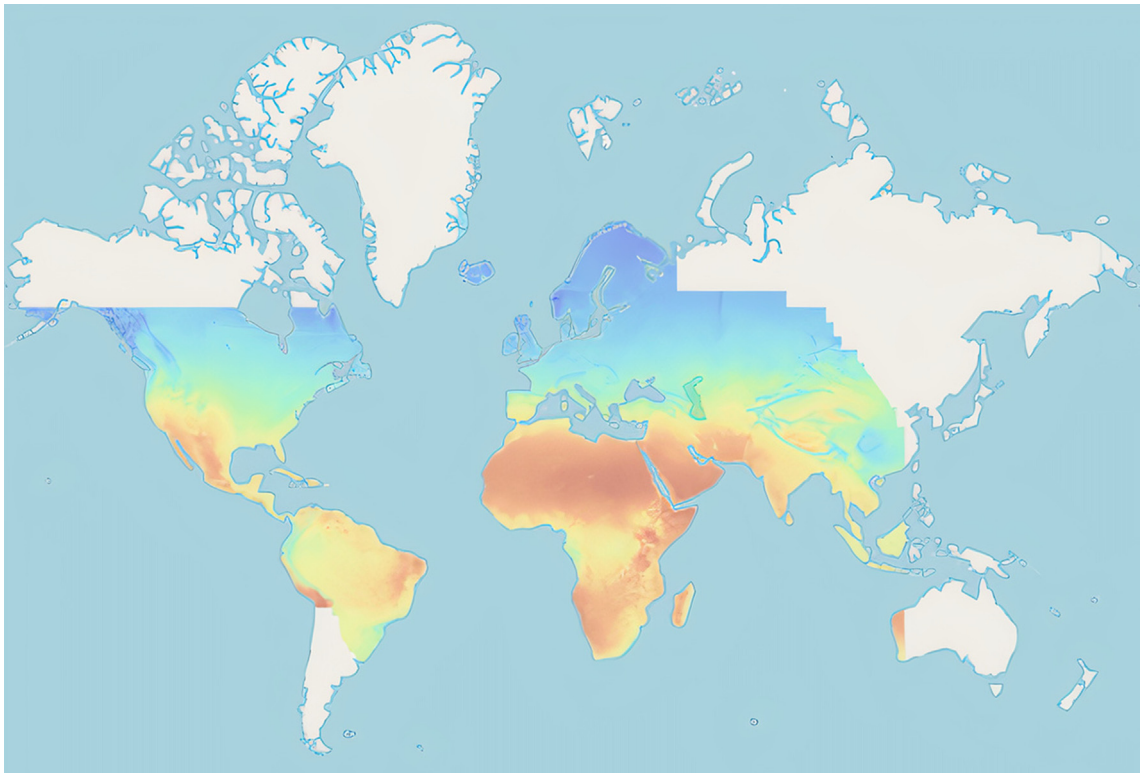

Figure 4. Locations with available TMY (EU) (https://re.jrc.ec.europa.eu/pvg_tools/en/tools.html).

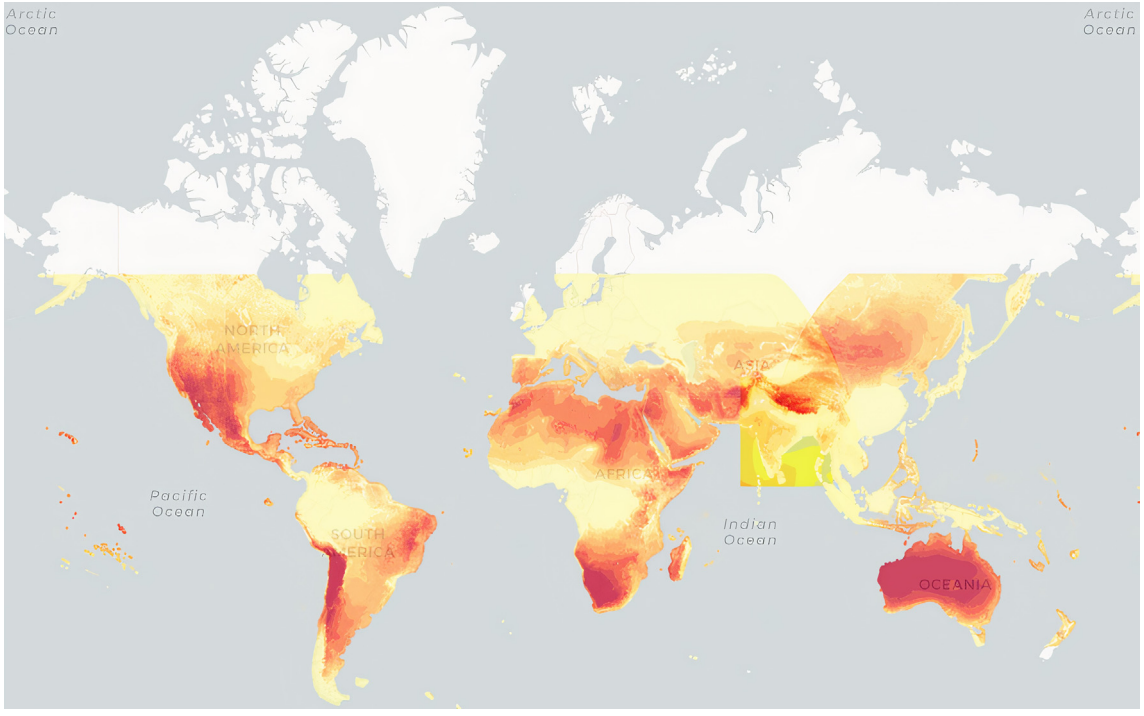

Figure 5. Locations with available TMY (USA) (https://maps.nrel.gov/nsrdb-viewer/).

annual average temperature, for the location of the SDHSTS. For the regions without available annual global solar radiation and annual average temperature, the latitude of the location is required, and the missing data are calculated as functions of the latitude. These interpolation functions were obtained for locations with available TMY to be used where these data are not available.

2. Material and method

2.1. Solar radiation on horizontal plane

For the locations without available TMY, the global solar radiation on horizontal plane (I_{gh}[kWh/m^2/year]) must be determined. Evaluation of

the global solar radiation on horizontal plane as a function of latitude but also of longitude was developed in [52] or as a function of latitude and other parameters such as sunshine duration, altitude, or relative humidity, was developed in [53]. In this study, an interpolation function was developed based on the available data from 144 randomly chosen locations, distributed worldwide.

These locations are situated, in 53 countries:

- from near the Equator (Macapa in Brazil at 0.034 °N) to beyond the polar circle (Murmansk in Russia at 68.972 °N) in the Northern hemisphere.
- from near the Equator (Quito in Ecuador at −0.206 °S) to near the southern limit of the region with available TMY (Montevideo in Uruguay at 34.874 °S).
- from East (Karratha in Australia at 116.845 °E) to West (Victoria in Canada at 123.366 °W).

Figure 6 presents the values of I_{gh} corresponding to the latitudes (λ [°]) of the considered locations and the proposed interpolation curve.

The following five interpolation functions were tested: Polynomial, Giddin, Lorentz, Pearson, and Gaussian, the last one being chosen because of the higher determination coefficient ($R^2 = 0.92295$). The Gaussian interpolation function is:

$$I_{gh} = I_{gh,0} + \frac{A \cdot e^{\frac{-4\cdot\ln(2)\cdot(\lambda-\lambda_c)^2}{w^2}}}{w \cdot \sqrt{\frac{\pi}{4\cdot\ln(2)}}} \quad (1)$$

with $I_{gh,0} = 470.83348 \pm 115.28132$, $\lambda_c = 18.07431 \pm 0.6716$, $A = 105131.156 \pm 14052.31537$ and $w = 59.30136 \pm 4.42576$. The latitude should be considered with the absolute (positive) value, regardless of whether the location is situated in the Northern or Southern hemisphere.

The relative errors of the estimations using Eq. (1) are within the range of −15.6 % and +25.8 %. Therefore, the interpolation should only be used in the preliminary sizing of the SDHSTS and only if more precise data is missing.

With this limited accuracy, the proposed interpolation function can be used for latitudes ranging in the interval of (0–70) °.

For the differences (x_i) between the global solar radiations on horizontal plane from the TMY and the global solar radiations on horizontal plane calculated with Eq. (1), the mean deviation (d [kWh/m^2/year]) was determined with the relation [54, 55]:

$$d = \frac{1}{n}\sum_{i=1}^{n}|x_i - m| \quad (2)$$

where m is the mean of the x_i data set.

The calculated value of the mean deviation for the global solar radiations on horizontal plane is 62.63639 kWh/m^2/year.

2.2. The annual average temperature

For the locations without available TMY, together with the global solar radiation, the annual average temperature (t [°C]) should also be determined, as it influences the efficiency of the STC.

Two ways to approximate the annual average temperature were tested:

1. as a function of only the latitude.
2. as a function of both latitude and altitude.

Finally, it was found that the maximum differences between the calculated and known annual average temperatures, are higher if the altitude is also taken into account, thus, only the latitude was considered. The variation of the annual average temperature as afunction of latitude was also presented in [56, 57]. Figure 7 presents the annual average temperatures corresponding to the latitudes of the considered locations and the proposed interpolation curve.

The following five interpolation functions were tested: Cubic, Farazdaghi-Harris, Langmuir, Boltzmann, and Logistic, the last one being chosen because of the higher determination coefficient ($R^2 = 0.924$). The Logistic interpolation function is:

$$t = A_2 + \frac{A_1 - A_2}{1 + \left(\frac{\lambda}{\lambda_0}\right)^p} \quad (3)$$

with $A_1 = 26.21664 \pm 0.64244$, $A_2 = 3.82782 \pm 1.46113$, $\lambda_0 = 39.61026 \pm 1.34957$ and $p = 4.81207 \pm 0.73361$.

The deviations between the calculated and the available TMY values are situated in the range of −4.23 °C and +5.37 °C. The interpolation should only be used for preliminary sizing, and if more precise data is missing.

As in the case of solar radiation estimation, considering the limited accuracy, the proposed interpolation function can be used for latitudes ranging in the interval of (0–70) °.

The value of the mean deviation for the annual average temperature, calculated with Eq. (2)is 0.951501 °C.

2.3. The annual global efficiency of the solar thermal collectors

The annual global efficiency (η_{col} [%]) is defined as:

$$\eta_{col} = \frac{Q_{ss}}{I_{gh}} \quad (4)$$

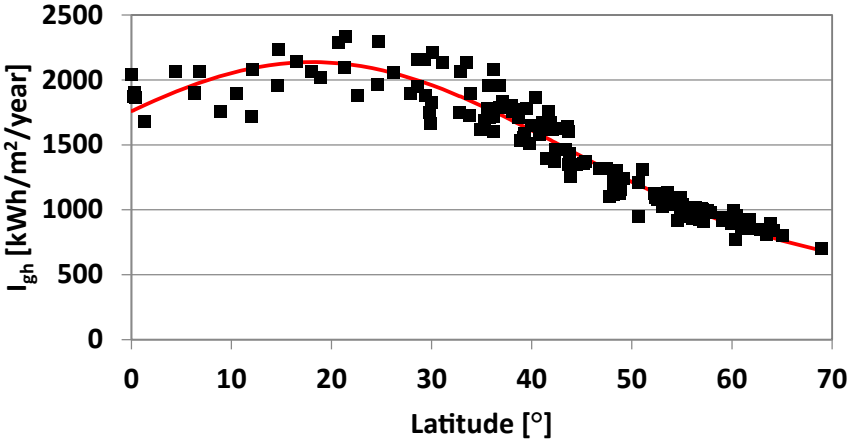

Figure 6. Global solar radiation on horizontal plane, as a function of latitude.

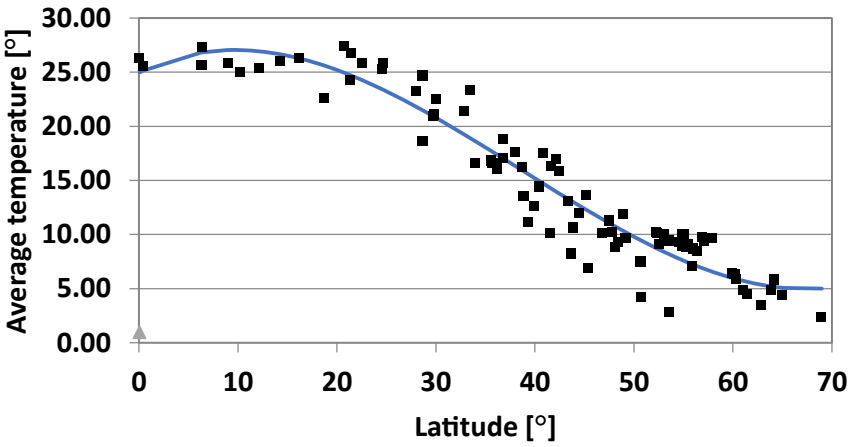

Figure 7. Annual average temperature, as function of latitude.

where Q_{ss} [kWh/m^2/year] is the specific heat produced by the STC in one year.

The values of the annual global efficiency, were determined for the following types of STC:

- Arcon-Sunmark HT-SolarBoost 35/10, a high performance flat STC and the most used in recent SDHSTSs built in Europe.
- Riomay Ecotube, a high performance evacuated STC.
- SEGS LS-2, a parabolic trough STC compatible with SDHSTS.

For the locations with available TMY, both (Q_{ss}) and (I_{gh}) required in Eq. (4) were calculated on an hourly basis. For each moment, the tilt angle between the solar beam and the plane of the collector, was determined based on an algorithm presented in [58, 59], that was already used and validated in previous studies at the Technical University of Cluj-Napoca, like [60, 61, 62]. This algorithm determines the following parameters: day angle; declination of the sun; equation of time; mean local time; solar time; hour angle of the sun; the angle of the solar altitude; the angle of the solar azimuth.

Taking into account the surface's tilt angle, the algorithm calculates the: solar angle of incidence; global solar radiation; direct normal radiation; diffuse normal radiation; reflected normal radiation.

For the parabolic trough STC, when the solar angle of incidence is calculated, the permanent movement of the STC determined by the solar tracking system is considered.

The instant efficiency for each of the flat and the evacuated STC is calculated as [58, 63, 64]:

$$\eta_{col} = \eta_0 - k_1\frac{\Delta t}{I_{gt}} - k_2\frac{\Delta t^2}{I_{gt}} \tag{5}$$

where η_0 [-] is the optical efficiency of the STC, k_1 [W/m^{2}K] and k_2 [W/m^{2}K^2] are correction coefficients, I_{gt} [W/m^2] is the global solar radiation on the tilted plane of the STC, Δt [°C] is the difference between the average temperature of the heat transfer fluid and the ambient temperature. It was considered that the behavior of STC is composed of successive steady states with the duration of one hour, the time step for TMY data.

To take into account the evolution over time of the flat STC quality, different values of the parameters corresponding to different periods of time were considered and presented in Table 6.

For the evacuated STC: $\eta_0 = 0.794$, $k_1 = 1.02$, and $k_2 = 0.0032$.

The calculations for the evacuated STCs, were conducted only for the single location where the characteristics of the existing SDHSTS could be identified, namely in Chemnitz, Germany. Even if, according to [1, 2], the majority of existing SDHSTSs in China are built with evacuated STCs, data related to these systems could not be found in the literature.

Table 6. The coefficients of Eq. (5) for flat STC.

Parameter	Before 2000	2000–2010	After 2010
η_0 [-]	0.775	0.785	0.838
k_1 [W/m^{2}K]	4.35	3.65	2.46
k_2 [W/m^{2}K^2]	0.0100	0.0170	0.0197

Since the difference between the average temperature of the heat transfer fluid and that of the ambient (Δt) is affecting the efficiency of the collector, the study investigates both high and low temperature STCs.

The two cases correspond to the situations of high and low temperatures of the central heating networks, and thus the average heat transfer fluid temperatures were set at 70 °C and 55 °C, respectively.

In this study, the tilt angle of the STC is considered to be equal with the latitude of the location, as recommended in [58, 64]. In [39] it is also mentioned that the optimum slope for the seasonal storage system is approximately equal to the latitude, while the optimum value for the short-term storage system is approximately equal to the latitude +15°.

The instant efficiency for the parabolic trough STC is calculated as [64]:

$$\eta_{col} = k_T \cdot IAM \cdot \eta_0 - k_1\frac{\Delta t}{DNI} - k_2\frac{\Delta t^2}{DNI} \tag{6}$$

where the new notations represent: k_T [-] is the correction coefficient, due to the transversal angle of incidence. Due to the solar tracking system, in this study $k_T = 1$. IAM [-] is the correction coefficient due to the longitudinal angle of incidence, also named incident angle modifier, DNI [W/m^2] is the direct beam solar radiation, or direct normal irradiance. For the considered parabolic trough STC: $\eta_0 = 0.733$, $k_1 = 0.0306$ and $k_2 = 0.00072$ [65].

The incident angle modifier was calculated with the equation [66]:

$$IAM = \cos(\theta) - 0.0003512 \cdot \theta - 0.0000317 \cdot \theta^2 \tag{7}$$

where θ [°] is the solar angle of incidence on the tilted plane of the parabolic trough STC. The orientation of the parabolic trough STC was considered North – South.

The calculations for the parabolic trough STC, were conducted only for the world's largest SDHSTS with this type of collector, located in Baotou, in the inner Mongolia, an autonomous region of China. From the solar heating energy point of view, this site is the second largest worldwide, after the one located in Silkeborg, Denmark. For this case study, the average heat transfer fluid temperatures in the STC were considered to be 250 °C and 180 °C for the high and low temperature regimes, respectively. Other four SDHSTSs with parabolic trough STC built in 2019, with

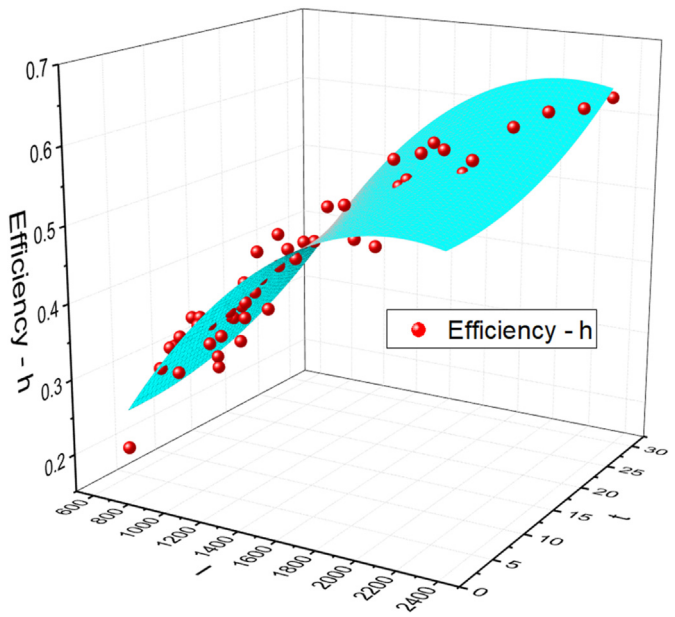

Figure 8. Annual global efficiency of the flat STC for high temperature regime.

a total surface area of 3876 m^2 are reported in [1], but no other data related to systems with these types of collectors could be found in the literature.

For the calculation of the annual global efficiency of the STC in the locations without available TMY, a correlation is proposed considering the variation of this parameter as a function of the global solar radiation on horizontal plane and of the annual average temperature, both considered in the location of the SDHSTS. To the best knowledge of the authors, such a dependency was proposed only in [67] to calculate the specific heat produced by the STC in one year, where a linear correlation available for I_{gh} = (873–1140) kWh/m^2/year and for t = (6.37–9.01) °C was developed.

In this study, considering larger availability ranges, more complex interpolation functions were investigated.

Figures 8 and 9 present the dependency of the annual global efficiency of the flat STC, as a function of the global solar radiation on horizontal plane and of the annual average temperature together with the proposed interpolation surface, for high and low heat transfer fluid temperature regimes.

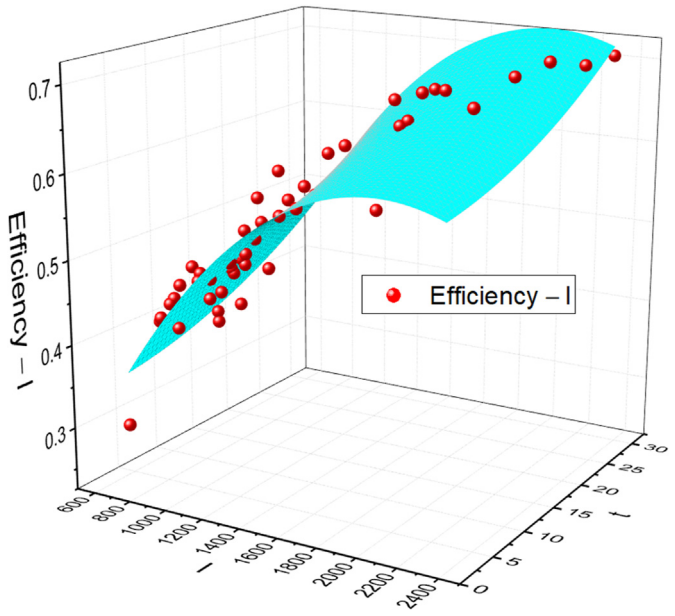

Figure 9. Annual global efficiency of the flat STC for low temperature regime.

In this case, an exponential and parabolic function were considered to fit de data set, with the latter proving to have the superior accuracy based on the R^2 coefficients. The values of the coefficients are R^2 = 0.933 and R^2 = 0.91 for high (70 °C) and low (55 °C) average operating temperatures, respectively. The Parabolic interpolation function is:

$$\eta_{col} = \eta_{col,0} + a \cdot I_{gt} + b \cdot t + c \cdot I_{gt}^2 + d \cdot t^2 \quad (8)$$

with the coefficients presented in Table 7 for both operating regimes of the STC.

The deviations between the calculated efficiencies and the corresponding values are within the ranges of (−10.8–19.1) % and (−10.1–16.1) %, for high and low operating temperatures, respectively. As in previous cases, it is suggested that interpolations only be used for preliminary sizing and only if more precise data is missing.

Interpolation functions for evacuated and parabolic trough STCs were not proposed, due to lack of data for validation.

2.4. The required aperture area of the STS

The annual specific heat yield of the STC (Q_{ss} [kWh/m^2/year]) (per unit surface area of aperture) is determined as:

$$Q_{ss} = \eta_{col} \cdot I_{gh} \quad (9)$$

This relation can be used for any location regardless of whether TMY is available or not, and thus if η_{col} and I_{gh} were determined exactly or by interpolation.

The aperture area (A [m^2]) can be determined as:

$$A = \frac{Q_s}{Q_{ss}} \quad (10)$$

where Q_s [kWh/year] is the annual global heat yield or the useful heat provided by the solar field.

This relation can also be used for any location, regardless of whether TMY is available or not. The value of Q_S depends on the annual heating demand of the consumers (Q_d) and on the SF.

2.5. The required volume of the STS

A critical parameter that must be determined is the ratio between the volume of the STS and the aperture area of the STC. This parameter is noted as RVA [m^3/m^2].

Figure 10 presents the distribution of the RVA as a function of the SF for:

- 17 existing systems build before 2000 in Austria, Denmark, Germany, Greece, and Sweden.
- 5 existing systems built during 2000–2010 in Canada (Okotoks/Drake Landing), Germany, and Sweden.
- 7 existing systems built after 2010 in China, Denmark, Germany, and Latvia.

Table 7. The coefficients of Eq. (8) for flat STC.

Operating regime	$\eta_{col,0}$	a	b	c	d
High temperature	−0.088	$5.91 \cdot 10^{-4}$	$-8.87 \cdot 10^{-4}$	$1.40 \cdot 10^{-7}$	$1.53 \cdot 10^{-4}$
Low temperature	0.027	$5.78 \cdot 10^{-4}$	$9.97 \cdot 10^{-4}$	$-143 \cdot 10^{-7}$	$1.06 \cdot 10^{-4}$

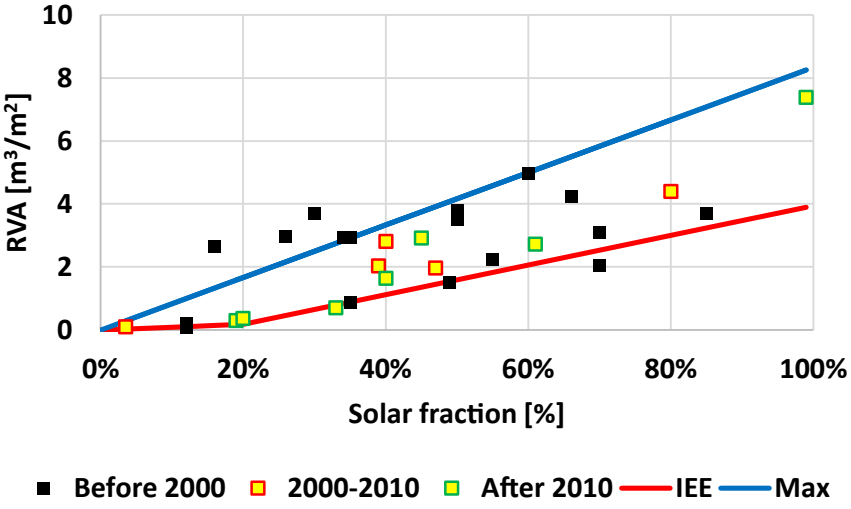

Figure 10. RVA [m^3/m^2] as a function of SF [%] at existing SDHSSTS.

The single recommendation for calculating the RVA as a function of the SF, identified in the literature, is indicated in [68]. This function is used in feasibility studies and is represented on Figure 10 as "IEE" with the red line (the proposed acronym comes from Intelligent Energy Europe/Solar District Heating guideline).

This correlation between the RVA and the SF is also implemented in the feasibility software SUNSTORE 4 [69]. It can be observed that almost all values of the existing systems' RVAs are equal or higher than the IEE recommendation.

The values of the RVA recommended by IEE can be calculated with the following relations:

$$\begin{aligned} RVA &= 0.9 \cdot SF \quad (\text{for } SF < 20\,\%) \\ RVA &= 4.7 \cdot SF - 0.7589 \quad (\text{for } SF \geq 20\,\%) \end{aligned} \tag{11}$$

A new relation was also proposed for the maximum RVA, represented on Figure 10 with the blue line and marked as "Max":

$$RVA = 8.33 \cdot SF \tag{12}$$

The relation for the maximum RVA, was proposed mainly to include most of the values corresponding to the older SDHSSTSs, newer systems achieve values closer to the IEE recommendations.

Thus, only few RVAs of existing systems remained outside the range between the recommended and the maximum values.

The large variation of the RVA can be explained by different particular conditions, an important one being the heat load profile of the heating network.

For example, if an STS is providing thermal energy not only for district heating but also for district cooling, large amounts of heat that should normally be stored will be transferred directly into the district cooling network, thus considerably lowering the required volume of the STS. On the other hand, if a SDHSSTS is located in a region with high amount of solar radiation and with low heat consumption during the summer, the required volume of the STS will increase considerably.

The volume of STS (V [m^3]) can be determined as a function of RVA and A [m^2]:

$$V = RVA \cdot A \tag{13}$$

2.6. The estimated costs

The estimated minimum and maximum specific investment costs corresponding to the ground mounted STC according to [68], together

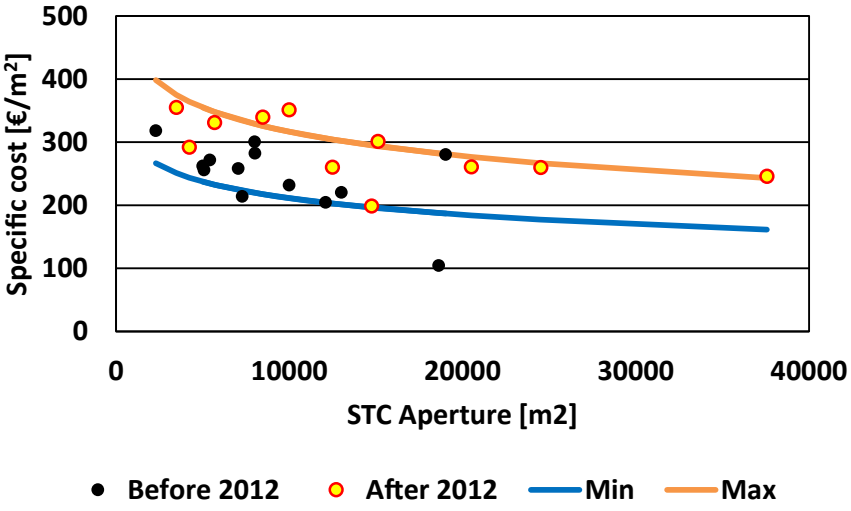

Figure 11. Minimum, maximum and reported specific investment costs of ground mounted STC.

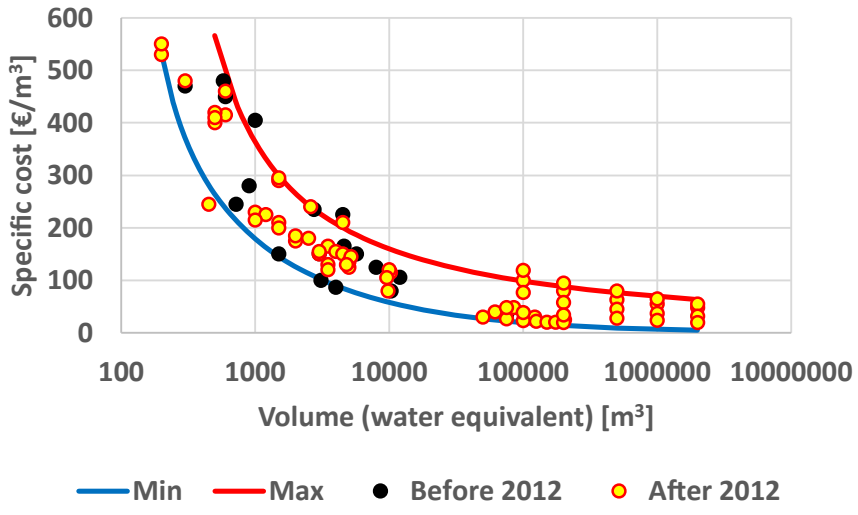

Figure 12. Minimum, maximum and reported specific investment costs of water equivalent STS volumes.

with the reported cost for existing systems built before2012, and after up to 2019, are presented in Figure 11.

It can be observed that the specific cost of the majority of the existing (older and newer) ground mounted STCs are situated between the recommended minimum and maximum values. The few specific costs not ranging in the recommended limit scan be explained by possible lower or higher prices of the land, by the higher or lower quality of the STC, or by particular mounting conditions that could lower or increase the specific cost. Inflation can also contribute to the increasing specific cost of newer systems.

By interpolating the "Min" and "Max" values, the following relations to calculate the minimum and maximum specific investment costs ($C_{min,S}$ [€/m^2] and $C_{max,S}$ [€/m^2]) of the ground mounted STCs are proposed:

$$C_{min,S} = 298.06 - 37.75 \cdot \ln\left(\frac{A}{1000}\right) \quad (14)$$

$$C_{max,S} = 444.55 - 55.57 \cdot \ln\left(\frac{A}{1000}\right) \quad (15)$$

These costs depend on the aperture area of the STC.

The specific investment costs corresponding to the water equivalent volume of the STSs according to [32], in comparison to the reported costs of simulated or existing systems built before 2012, are presented in Figure 12.

It can be observed that most of the newer STS specific costs are situated inside the minimum and maximum values recommended in [70] and that many new systems are characterized by higher volumes than the ones of the systems built before 2012.

For the minimum and maximum specific investment costs corresponding to the STS water equivalent volume, the following four interpolation functions were tested: Exponential, Allometric, Belehradek, and Farazdaghi-Harris.

The functions were chosen based on the highest value of the determination coefficient as follows:

- Belehradek interpolation function for the minimum specific cost ($R^2 = 0.997$)

$$C_{min,V} = a \cdot (V - b)^c \ [€/m^3] \quad (16)$$

where $a = 4290.03 \pm 339.24$, $b = 112.82 \pm 9.12$, and $c = -0.47 \pm 0.01$.

- Farazdaghi-Harris for the maximum specific cost ($R^2 = 0.999$)

$$C_{max,V} = (a + b\ V^c)^{-1} \ [€/m^3] \quad (17)$$

where $a = -0.029 \pm 0.007$, $b = 0.023 \pm 0.007$, and $c = -0.045 \pm 0.001$.

2.7. The scheme of the calculation algorithm

Based on the presented equations, Figure 13 shows the flow chart of the preliminary sizing algorithm.

There are two differences between the calculations based on the TMY data and the ones based on interpolation.

The first difference is that I_{gh} and t are taken from the TMY data, however if such data is unavailable then the interpolation functions from Eqs. (1) and (3) are used.

The second difference consists in the evaluation of STC efficiency.

- η_{col} is computed on an hourly basis with one of the Eqs. (5) and (6) or 7) depending on the type of STC if TMY is available.
- η_{col} is computed with the Eq. (8) if the interpolation function must be used.

The sections of the algorithm that employ the TMY or the interpolation equations are outlined with black and red, respectively.

3. Results

The proposed method for preliminary sizing of SDHSSTSs was tested for 10 existing systems, built with flat STC in Europe during (2013–2019) for which data related to efficiency, STCaperture area and STSstorage volume are available. The single large system located on the Northern American continent, built in 2008 was found in Okotoks (Drake Landing), Canada with flat STCs, and was also investigated. The single systems equipped with evacuated STCs and parabolic trough STCs, for which data could be identified, were built in 2000 in Chemnitz, Germany and in 2017 in Baotou, China, respectively and were also subject to investigation within this study. Calculations were also performed for the system built with flat STCsin 2017 in Beijing, China where TMY is not available.

The comparative results related to the efficiency of the STC, aperture area of the STC and water equivalent storage volume are presented in Tables 8, 9, and 10, respectively.

If the calculations are made based on the available TMY (except Beijing, case in which such calculations are not possible), it can be observed that:

- In 13 of 19 cases (68.4 % of cases), the efficiency of the existing systems is situated between the efficiencies corresponding to high and low temperature regimes.

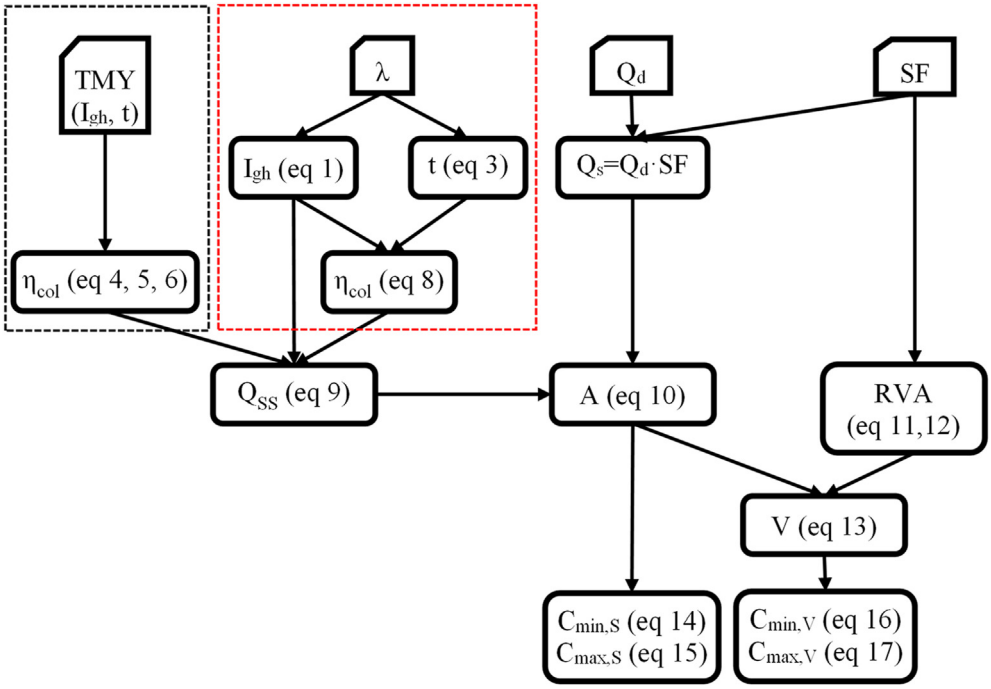

Figure 13. Flow chart of the preliminary sizing algorithm.

Table 8. The comparative efficiencies of the existing and calculated systems.

No.	Location	η [%]	$\eta_{HT,TMY}$ [%]	$\eta_{LT,TMY}$ [%]	Status TMY	$\eta_{HT,int}$ [%]	$\eta_{LT,int}$ [%]	Status int.
1	Vojens	42.3%	35.0%	46.2%	✓	37.5%	48.4%	✓
2	Zhongba	48.3%	44.8%	56.0%	✓	58.7%	68.0%	×
3	Büsingen	43.5%	42.6%	53.4%	✓	45.3%	55.8%	×
4	Dronninglund	39.7%	36.9%	48.0%	✓	35.5%	46.5%	✓
5	Nykobing	45.3%	38.2%	49.2%	✓	36.8%	47.7%	✓
6	Gram	42.8%	35.3%	46.4%	✓	37.5%	48.3%	✓
7	Silkeborg	51.5%	36.4%	47.5%	×	36.4%	47.5%	×
8	Trustrup-Lyngby	54.4%	37.3%	48.2%	×	36.4%	47.3%	×
9	Salaspils	57.4%	35.5%	46.5%	×	35.9%	46.8%	×
10	La Parreña	32.9%	56.5%	65.3%	×	58.1%	67.5%	×
11	Okotoks	28.7%	27.4%	34.3%	✓	42.2%	52.9%	×
12	Baotou	55.2%	53.8%	64.1%	✓	-	-	-
13	Chemnitz	42.8%	36.3%	47.3%	✓	-	-	-
14	Beijing	50.3%	-	-	-	52.3%	62.4%	✓
15	Ingelstad	34.9%	26.6%	35.4%	✓	36.0%	46.9%	×
16	Kungälv	41.9%	33.2%	4290.0%	✓	34.8%	45.8%	✓
17	Herlev	43.5%	30.0%	39.2%	✓	37.0%	47.0%	✓
18	Gaziantep	45.2%	44.7%	52.7%	✓	54.4%	64.3%	×
19	Steinfurt	20.6%	37.5%	48.9%	×	40.7%	51.5%	×
20	Eggenstein	27.4%	37.7%	47.7%	×	43.9%	54.5%	×

η [%] is the efficiency of the existing STC;
$\eta_{HT,TMY}$ [%] is the efficiency of the STC at high temperature regime, calculated based on the available TMY;
$\eta_{LT,TMY}$ [%] is the efficiency of the STC at low temperature regime, calculated based on the available TMY;
$\eta_{HT,int}$ [%] is the efficiency of the STC at high temperature regime, calculated based on interpolation;
$\eta_{LT,int}$ [%] is the efficiency of the STC at low temperature regime, calculated based on interpolation;
Status TMY and Status int (interpolations): "✓" = OK; "×" = Fail.

- In 6 of 19 cases (31.6 % of cases), the efficiency of the existing systems is situated outside the efficiencies corresponding to high and low temperature regimes.

The calculations based on interpolations were not performed in the cases of the evacuated STCs and parabolic trough STCs, because no interpolation functions were determined for these types of collectors.

Table 9. The comparative aperture areas of the existing and calculated STCs.

No.	Location	A [m^2]	$A_{HT,TMY}$ [m^2]	$A_{LT,TMY}$ [m^2]	Status TMY	$A_{HT,int}$ [m^2]	$A_{LT,int}$ [m^2]	Status int.
1	Vojens	69500	83735	63616	✓	71835	55711	✓
2	Zhongba	34650	37313	29851	✓	17331	14959	×
3	Büsingen	1090	1114	888	✓	956	776	×
4	Dronninglund	37573	40431	31056	✓	43478	33259	✓
5	Nykobing	20084	23791	18488	✓	25714	19834	✓
6	Gram	44800	54303	41309	✓	47409	36747	✓
7	Silkeborg	156694	221607	169851	×	218579	168421	×
8	Trustrup-Lyngby	7245	10588	8173	×	11086	8538	×
9	Salaspils	21595	34884	26608	×	34091	26144	×
10	La Parreña	6270	3658	3163	×	3929	3382	×
11	Okotoks	2307	2435	1965	✓	3000	2398	×
12	Baotou	93000	95354	80032	✓	-	-	-
13	Chemnitz	540	637	488	✓	-	-	-
14	Beijing	10834	-	-	-	9893	8284	×
15	Ingelstad	1425	1871	2235	✓	1299	998	×
16	Kungälv	11000	13886	10471	✓	13595	10369	✓
17	Herlev	1025	1487	1137	×	1263	977	✓
18	Gaziantep	4000	4044	3431	✓	3539	2994	×
19	Steinfurt	510	280	215	×	239	189	×
20	Eggenstein	1000	816	645	×	590	475	×

A [m^2] is the aperture area of the existingSTC;
$A_{HT,TMY}$ [m^2] is the aperture area of the STC at high temperature regime, calculated based on the available TMY;
$A_{LT,TMY}$ [m^2] is the aperture area of the STC at low temperature regime, calculated based on the available TMY;
$A_{HT,int}$ [m^2] is the aperture area of the STC at high temperature regime, calculated based on interpolation;
$A_{LT,int}$ [m^2] is the aperture area of the STC at low temperature regime, calculated based on interpolation;
Status TMY and Status int (interpolations): "✓" = OK; "×" = Fail.

Table 10. The comparative water equivalent storage volumes of the existing and calculated STCs.

No.	Location	V [m^3]	$V_{HT,TMY}$ [m^3]	$V_{LT,TMY}$ [m^3]	Status TMY	$V_{HT,int}$ [m^3]	$V_{LT,int}$ [m^3]	Status int.
1	Vojens	203000	86270	313881	✓	75550	269273	✓
2	Zhongba	1000	92359	261525	×	51924	129931	×
3	Büsingen	NA	108	1253	-	94	1075	-
4	Dronninglund	61700	34817	134716	✓	37287	144869	✓
5	Nykobing	6000	3161	37654	✓	3392	40698	✓
6	Gram	122000	87084	275930	✓	77466	240899	✓
7	Silkeborg	256000	30760	369197	✓	30501	364153	✓
8	Trustrup-Lyngby	2800	5321	26459	×	5559	27704	×
9	Salaspils	8000	4819	58117	✓	4735	56796	✓
10	La Parreña	660	6222	17673	×	6653	18983	×
11	Okotoks	10156	5897	16227	✓	7197	19992	✓
12	Baotou	66000	63393	262118	✓	-	-	-
13	Chemnitz	1955	774	1708	×	-	-	-
14	Beijing	80000	-	-	-	32648	82409	✓
15	Ingelstad	5000	2977	5851	✓	1587	5417	✓
16	Kungälv	1000	437	3132	✓	311	3943	✓
17	Herlev	3000	1318	3315	✓	870	3688	✓
18	Gaziantep	13000	12705	23724	✓	9401	24454	✓
19	Steinfurt	1000	235	609	×	159	676	×
20	Eggenstein	3000	915	2148	×	532	1965	×

V [m^3] is the storage volume of the existing STC;
$V_{HT,TMY}$ [m^3] is the storage volume of the STC at high temperature regime, calculated based on the available TMY;
$V_{LT,TMY}$ [m^3] is the storage volume of the STC at low temperature regime, calculated based on the available TMY;
$V_{HT,int}$ [m^3] is the storage volume of the STC at high temperature regime, calculated based on interpolation;
$V_{LT,int}$ [m^3] is the storage volume of the STC at low temperature regime, calculated based on interpolation;
Status TMY and Status int (interpolations): "✓" = OK; "×" = Fail.

Based on the interpolations, it can be observed that:

- In 7 of 18 cases (38.9 % of cases), the efficiency of the existing systems is situated between the efficiencies corresponding to high and low temperature regimes.
- In 11 of 18 cases (61.1 % of cases), the efficiency of the existing systems is situated outside the efficiencies corresponding to high and low temperature regimes.

From calculations conducted based on the TMY, the aperture area of existing systems is:

- Situated between the values corresponding to high and low temperature regimes, in 12 of 19 cases (63.2 % of cases).
- Situated outside the values corresponding to high and low temperature regimes, in 7 of 19 cases (36.8 % of cases).

Based on the estimations that were conducted using interpolations, the aperture area of existing systems is:

- Situated between the values corresponding to high and low temperature regimes, in 6 of 18 cases (33.3 % of cases).
- Situated outside the values corresponding to high and low temperature regimes, in 12 of 18 cases (66.7 % of cases).

In the case of the system from Büsingen, Germany, the storage volume of the existing system is not available, and comparisons could not be made for this system.

By employing the TMY, the results show that the storage volume of the existing systems is:

- Within the minimum and maximum calculated values, for 12 of 18 cases (66.7 % of cases).
- Outside the minimum and maximum calculated values, for 6 of 18 cases (33.3 % of cases).

From the interpolations, the storage volume of the existing systems is:

- Within the minimum and maximum calculated values, for 12 of 17 cases (70.6 % of cases).
- Outside the minimum and maximum calculated values, for 5 of 17 cases (29.4 % of cases).

By comparing the calculated and the existing characteristic parameters of the SDHSSTS, the number of cases in which the values were reasonably determined, based on the available TMY, are as follows:

- The efficiency of the STC in over 68 % of cases
- The aperture area in over 63 % of cases
- The storage volume in over 66 % of cases.

The interpolations yielded accurate values for:

- the efficiency of the systems in almost 40% of cases
- the aperture area in over 33 % of cases
- the storage volume in over 70 % of cases.

From the obtained data, it can be observed that the calculations based on available TMY are more precise in comparison to the calculations based on interpolations.

Even in the case of the storage volume, where the percentage of correct calculations is higher based on interpolations, the number of plants with correct estimation is similar for both methods. The percentage of correct calculations is higher for the interpolations-based method, only because the number of plants for which these calculations were performed is lower, considering that interpolations could not be performed for the plants with evacuated STCs (Chemnitz) and with parabolic trough STCs (Baotou).

4. Conclusions

The study presents in detail a preliminary sizing method of the SDHSSTS. Such a method is missing from the literature.

The proposed method can provide initial values of the aperture area of the STC and of the storage volume, as these are the most important parameters of such systems but should be always followed by more accurate analysis on their dynamic behavior. Such an analysis will be able to determine the design values of the aperture area and of the storage volume.

For the locations with available TMY, the calculations are expected to provide correct estimations: for the efficiency of the STC in over 68 % of cases, for the aperture area in over 63 % of cases and for the storage volume in over 66 % of cases. For the locations without available TMY, the calculations based on interpolations are expected to provide correct estimations: for the efficiency of the STC in almost 40 % of cases, for the aperture area in over 33 % of cases and for the storage volume in over 70 % of cases.

It was highlighted that the calculations should be based on available TMY and the interpolations should be used only in the absence of such data. For the detailed calculation of the SDHSSTS, the use of measured data for a period of at least one year is recommended.

The errors of the interpolation equations were determined as follows:

- For the global solar radiation on horizontal plane in the range of (−15.6 … +25.8) %.
- For the annual average temperatures in the range of (−4.23 … +5.37) °C.
- For the annual global efficiency of the STC in the range of (−10.8 … 19.1) %.

Considering the limited accuracy, the interpolation functions are valid in the range of I_{gh}= (704–2337) kWh/m^2/year and t=(2–30) °C.

By consequence, the STC annual global efficiency, the STC aperture area and the STS storage volume can also be computed within the same validity range.

For the calculation of the cost estimations of both STC and STS, interpolation functions, determined based on references from 2012 were used, however it was proven that these functions are still valid for systems built or simulated in recent years.

Declarations

Author contribution statement

Daniel P. Hiris, Octavian G. Pop, Mugur C. Balan: Conceived and designed the experiments; Performed the experiments; Analyzed and interpreted the data; Contributed reagents, materials, analysis tools or data; Wrote the paper.

Funding statement

This work was supported by the Project “Entrepreneurial competences and excellence research in doctoral and postdoctoral programs – ANTREDOC no. 56437/24.07.2019”, project co-funded by the European Social Fund.

Data availability statement

Data included in article/supp. material/referenced in article.

Declaration of interests statement

The authors declare no conflict of interest.

Additional information

No additional information is available for this paper.

References

[1] W. Weiss, M. Spörk-Dür, Solar heat worldwide. Global market development and trends in 2019, in: Detailed Market Data 2018, AEE - Institute for Sustainable Technologies, Austria, IEA Solar Heating & Cooling Programme, 2020.

[2] D. Tschopp, Z. Tian, M. Berberich, J. Fan, B. Perers, S. Furbo, Large-scale solar thermal systems in leading countries: a review and comparative study of Denmark, China, Germany and Austria, Appl. Energy 270 (2020) 114997.

[3] Solarthermalworld.org, 2021. https://www.solarthermalworld.org/. (Accessed 10 November 2021).

[4] Major solar district heating project in China, 2021. https://www.euroheat.org/news/industry-news/major-solar-district-heating-project-china/. (Accessed 10 November 2021).

[5] Solare Grossanlagen von Ritter XL Solar, 2021. https://www.ritter-xl-solar.de/. (Accessed 10 November 2021).

[6] EUDP, Long term storage and solar district heating, in: A Presentation of the Danish Pit and Borehole thermal Energy Storages in Brædstrup, Marstal, Dronninglund and Gram, 2021. https://ens.dk/sites/ens.dk/files/Forskning_og_udvikling/sol_til_fjernvarme_brochure_endelig.pdf. (Accessed 10 November 2021).

[7] Arcon-Sunmark, Record-breaking Solar Heating System Ready on Time, 2017. https://www.euroheat.org/news/record-breaking-solar-heating-system-ready-time/. (Accessed 10 November 2021).

[8] F. Galatoulas, M. Frere, C.S. Ioakimidis, An overview of renewable smart district heating and cooling applications with thermal storage in Europe, in: Proceedings of the 7th International Conference on Smart Cities and Green ICT Systems (SMARTGREENS 2018), 2018, pp. 311–319.

[9] Large-Scale Solar Thermal Projects, 2021. https://www.greenonetec.com/geschaeftsfelder/grossprojekte/. (Accessed 10 November 2021).

[10] Solar Thermal district heating plant with Biomass boiler house in Latvia, Salaspils, 2021. https://www.filter.eu/en/experiences/solar-thermal-district-heating-plant-with-biomass-boiler-house-in-latvia-salaspils. (Accessed 10 November 2021).

[11] Filter SIA & Arcon-Sunmark A/S, Solar thermal District Heating Plant, Inauguration Event – SalaspilsSiltums, Latvia, 2019. https://www.hyxo.ru/images/PRESS/Salaspils_Siltums_Inauguration_Event_Report-12092019-v2.pdf. (Accessed 10 November 2021).

[12] M. Guadalfajara, M.A. Lozano, L.M. Serra, Analysis of large thermal energy storage for solar district Heating,Conference: eurotherm seminar #99, in: Advances in Thermal Energy Storage, Lleida, Spain, 2014.

[13] D. Mangold, T. Schmidt, V. Lottner, Seasonal thermal energy storage in Germany, in: Proc. of Futurestock, Warschau, 2003.

[14] D. Bauer, R. Marx, J. Nußbicker-Lux, F. Ochs, W. Heidemann, H. Müller-Steinhagen, German central solar heating plants with seasonal heat storage, Sol. Energy 84 (2010) 612–623.

[15] C. Bott, I. Dressel, P. Bayer, State-of-technology review of water-based closed seasonal thermal energy storage systems, Renew. Sustain. Energy Rev. 113 (2019) 109241.

[16] Asia Development Bank, Solar District Heating in the People's Republic of China.Status and Development Potential, 2019. https://www.adb.org/sites/default/files/publication/514916/solar-district-heating-peoples-republic-china.pdf. (Accessed 10 November 2021).

[17] J.O. Dalenbaeck, Central Solar Heating Plants with Seasonal Storage - Status Report, 1990. https://citeseerx.ist.psu.edu/viewdoc/download?doi=10.1.1.470.6729&rep=rep1&type=pdf. (Accessed 10 November 2021).

[18] J.O. Dalenbäck, European Large-Scale Solar Heating Network. http://www.hvac.chalmers.se/cshp. (Accessed 10 November 2021).

[19] G.K. Pavlov, B.W. Olesen, Seasonal ground solar thermal energy storage-review of systems and applications, in: Proceedings, APA, 2011, pp. 1–2.

[20] A. Hesaraki, S. Holmberg, F. Haghighat, Seasonal thermal energy storage with heat pumps and low temperatures in building projects—a comparative review, Renew. Sustain. Energy Rev. 43 (2015) 1199–1213.

[21] Sun & Wind Energy. The Platform for Renewable Energy, 2021. https://www.sunwindenergy.com/. (Accessed 10 November 2021).

[22] B. Morvaj, R. Evins, J. Carmeliet, Optimising urban energy systems: simultaneous system sizing, operation and district heating network layout, Energy 116 (2016) 619–636.

[23] M. Pavičević, T. Novosel, T. Pukšec, N. Duić, Hourly optimization and sizing of district heating systems considering building refurbishment – case study for the city of Zagreb, Energy 137 (2017) 1264–1276.

[24] K. Narula, F.D.O. Filho, J. Chambers, M.K. Patel, Simulation and comparative assessment of heating systems with tank thermal energy storage – a Swiss case study, J. Energy Storage 32 (2020) 101810.

[25] M. Salvestroni, G. Pierucci, A. Pourreza, F. Fagioli, F. Taddei, M. Messeri, M. de Lucia, Design of a solar district heating system with seasonal storage in Italy, Appl. Therm. Eng. 197 (2021) 117438.

[26] B.R. Knudsen, D. Rohde, H. Kauko, Thermal energy storage sizing for industrial waste-heat utilization in district heating: a model predictive control approach, Energy 234 (2021) 121200.

[27] S. Qiu, M. Ruth, S. Ghosh, Evacuated tube collectors: a notable driver behind the solar water heater industry in China, Renew. Sustain. Energy Rev. 47 (2015) 580–588.

[28] J. Huang, Z. Tian, J. Fan, A comprehensive analysis on development and transition of the solar thermal market in China with more than 70% market share worldwide, Energy 174 (2019) 611–624.

[29] P. Olczak, D. Matuszewska, J. Zabagło, The comparison of solar energy gaining effectiveness between flat plate collectors and evacuated tube collectors with heat pipe: case study, Energies 13 (2020) 1829.

[30] S. Faisal Ahmed, M. Khalid, M. Vaka, R. Walvekar, A. Numan, A. Khaliq Rasheed, N. Mujawar Mubarak, Recent progress in solar water heaters and solar collectors: a comprehensive review, Therm. Sci. Eng. Prog. 25 (2021) 100981.

[31] F. Ochs, W. Heidemann, H. Müller-Steinhagen, Performance of Large-scale seasonal thermal energy stores, J. Solar Energy Eng. Transact. ASME 131 (2009) 0410051–0410057.

[32] A.V. Novo, J.R. Bayon, D. Castro-Fresno, J. Rodriguez-Hernandez, Review of seasonal heat storage in large basins: water tanks and gravel–water pits, Appl. Energy 87 (2010) 390–397.

[33] A. Dahash, F. Ochs, M.B. Janetti, W. Streicher, Advances in seasonal thermal energy storage for solar district heating applications: a critical review on large-scale hot-water tank and pit thermal energy storage systems, Appl. Energy 239 (2019) 296–315.

[34] S.A. Klein, W.A. Beckman, J.A. Duffie, A design procedure for solar heating systems, Sol. Energy 18 (1976) 113–127.

[35] F. Hooper, C. Attwater, A. Brunger, R. Cook, J. McClenahan, Solar Space Heating Systems Using Annual Heat Storage, Progress report, 1978. July 1 - December 30, 1977, Argonne, IL (United States).

[36] P.J. Lunde, Prediction of the performance of solar heating systems utilizing annual storage, Sol. Energy 22 (1979) 69–75.

[37] M.S. Drew, R.B.G. Selvage, Sizing procedure and economic optimization methodology for seasonal storage solar systems, Sol. Energy 25 (1980) 79–83.

[38] F. Baylin, S. Sillman, Systems Analysis Techniques for Annual Cycle thermal Energy Storage Solar Systems, Golden, Colorado, USA, 1980.

[39] J.E. Braun, S.A. Klein, J.W. Mitchell, Seasonal storage of energy in solar heating, Sol. Energy 26 (1981) 403–411.

[40] T. Schmidt, L. Deschaintre, Solar District Heating (SHD) Online-Calculator. Calculation Program for the Cost-Benefit Analysis of Solar District Heating Systems, 2013. https://sdh-online.solites.de/Content/media/SDH-Online-Calculator.PDF. (Accessed 8 November 2021).

[41] M. Guadalfajara, M.A. Lozano, L.M. Serra, Comparison of simple methods for the design of central solar heating plants with seasonal storage, Energy Proc. 48 (2014) 1110–1117.

[42] M. Guadalfajara, M.A. Lozano, L.M. Serra, A simple method to calculate central solar heating plants with seasonal storage, Energy Proc. 48 (2014) 1096–1109.

[43] M. Guadalfajara, M.A. Lozano, L.M. Serra, Simple calculation tool for central solar heating plants with seasonal storage, Sol. Energy 120 (2015) 72–86.

[44] M. Guadalfajara, Economic and Environmental Analysis of central Solar Heating Plants with Seasonal Storage for the Residential Sector, Doctoral Thesis, University of Zaragoza, Zaragoza, Spain, 2016.

[45] M. Guadalfajara, M.A. Lozano, L.M. Serra, Geographic evaluation of central solar heating plants with seasonal storage for the residential sector in Europe, in: Conference Paper: 14th International Symposium on District Heating and Cooling, Stockholm, Sweden, 2014.

[46] B. McDaniel, D. Kosanovic, Modeling of combined heat and power plant performance with seasonal thermal energy storage, J. Energy Storage 7 (2016) 13–23.

[47] X. Li, Z. Wang, J. Li, M. Yang, G. Yuan, Y. Bai, L. Chen, T. Xu, A. Gilmanova, Comparison of control strategies for a solar heating system with underground pit seasonal storage in the non-heating season, J. Energy Storage 26 (2019) 100963.

[48] A. Rosato, A. Ciervo, G. Ciampi, M. Scorpio, S. Sibilio, Impact of seasonal thermal energy storage design on the dynamic performance of a solar heating system serving a small-scale Italian district composed of residential and school buildings, J. Energy Storage 25 (2019) 100889.

[49] D.Y. Goswami, Principles of Solar Engineering, 2015.

[50] T. Huld, PVMAPS: software tools and data for the estimation of solar radiation and photovoltaic module performance over large geographical areas, Sol. Energy 142 (2017) 171–181.

[51] M. Sengupta, Y. Xie, A. Lopez, A. Habte, G. Maclaurin, J. Shelby, The national solar radiation data base (NSRDB), Renew. Sustain. Energy Rev. 89 (2018) 51–60.

[52] H. Anas, Y. elMghouchi, Y. Halima, A. Nawal, C. Mohamed, Novel climate classification based on the information of solar radiation intensity: an application to the climatic zoning of Morocco, Energy Convers. Manag. 247 (2021) 114770.

[53] R.G. Makade, S. Chakrabarti, B. Jamil, Prediction of global solar radiation using a single empirical model for diversified locations across India, Urban Clim. 29 (2019) 100492.

[54] R.E. Shiffler, P.D. Harsha, Upper and lower bounds for the sample standard deviation, Teach. Stat. 2 (1980) 84–86.

[55] F. Hampel, Mean Deviation, Encyclopedia of Biostatistics, John Wiley & Sons, Ltd., 2005.

[56] W.D. Sellers, Physical climatology, 1965, p. 272.

[57] Gerald North, Theory of energy-balance climate models, J. Atmos. Sci. 32 (1975) 2033–2043. https://journals.ametsoc.org/view/journals/atsc/32/11/1520-0469_1975_032_2033_toebcm_2_0_co_2.xml. (Accessed 10 November 2021).

[58] J. Duffie, W.A. Beckman, Solar Engineering of thermal Processes, second ed., Wiley, New York, USA, 1980.

[59] V. Quaschning, Understanding Renewable Energy System, Earthscan, London, 2007.

[60] P.V. Unguresan, R.A. Porumb, D. Petreus, A.G. Pocola, O.G. Pop, M.C. Balan, Orientation of facades for active solar energy applications in different climatic conditions, J. Energy Eng. 143 (2017) 4017059.

[61] A.C. Abrudan, O.G. Pop, A. Serban, M.C. Balan, New perspective on performances and limits of solar fresh air cooling in different climatic conditions, Energies 12 (2019) 2113.
[62] P.D. Hiris, F. Bode, O.G. Pop, M.C. Balan, Simple modeling of the solar seasonal thermal storage behavior, in: I. Visa, A. Duta (Eds.), Solar Energy Conversion in Communities, Proceedings of the Conference for Sustainable Energy (CSE), Springer Proceedings in Energy, Springer, Cham, 2020, pp. 21–34.
[63] ISO 9806:2013 - Solar Energy — Solar thermal Collectors — Test Methods, 2013.
[64] S.A. Kalogirou, Solar Energy Engineering. Processes and Systems, second ed., Elsevier, Amsterdam, The Netherlands, 2014.
[65] O.G. Pop, A.M. Magurean, A.G. Pocola, M. Ciocan, A. Zaaoumi, M.C. Balan, Performances of Solar Thermal Collectors in Different Climatic Conditions, Springer Tracts in Civil Engineering, 2021, pp. 235–273.
[66] V.E. Dudley, G.J. Kolb, A.R. Mahoney, T.R. Mancini, C.W. Matthews, M. Sloan, D. Kearney, Test Results: SEGS LS-2 Solar Collector, 1994.
[67] M. Zukowski, P. Radzajewska, A new method to determine the annual energy output of liquid-based solar collectors, Proceedings 16 (2019) 39.
[68] Intelligent Energy Europe (IEE), Solar District Heating Guidelines, 2012. https://www.euroheat.org/wp-content/uploads/2016/04/SDHtake-off_SDH_Guidelines.pdf. (Accessed 8 November 2021).
[69] SUNSTORE 4, Project Final Report, 2014. https://www.euroheat.org/wp-content/uploads/2016/04/SUNSTORE4_Report.pdf. (Accessed 8 November 2021).
[70] D. Mangold, O. Miedaner, E.P. Tziggili, T. Schmidt, M. Unterberger, B. Zeh, Technisch-wirtschaftlicheanalyse und weiterentwickling der solarenlangzeit-wärmespeicherung, Forschungberichtzum BMU-Vorhaben 0329607N, 2012.